

A deep learning approach to sign language recognition using stacked autoencoders and neural networks

Pablo Rivas

Jan/24/17

1 Introduction

Language is an essential part of being human as it enables us to communicate with others. Some people have to develop additional means of communication for different reasons. A popular alternative language is through signs. This type of language is based on symbols or figures produced using the hands.

Sign language recognition is a task that has been studied in the last few years [13]. We believe this is an important problem to address because it directly affects the quality of life of people who need to communicate using sign language. The task is to develop algorithms that can recognize different signs in an alphabet and that can do so in an efficient manner. Ideally, the methodologies should be fast to the point of enabling the near real-time processing of signs [12].

In this research we deal with the recognition of signs over the american sign language (ASL). The proposed approach uses depth images of subjects making different signs, building upon the work of B. Kang, et.al. in [5].

Typical approaches involve the using hidden Markov models [12], and a combination of them with other discriminative functions for feature extraction in multi-stage architectures [7]. Other major alternatives included the exploration of neural strategies combined with fuzzy systems [1]. For a more detaile review of alternatives for generic hand gesture recognition we can turn to the work in [9].

However, with the dramatic attention that deep learning has gained recently in the machine learning and the image processing for pattern recognition communities, we are motivated to similarly explore this new algorithmic alternative to see if it offers better solutions to open problems. Most recently, the authors in [5] have explored a deep learning approach based on convolutional neural networks (CNNs) achieving outstanding results. The research presented here also explores a novel deep learning approach but based in autoencoders and neural networks. We will show that this alternative approach achieves great performance and efficiency.

The rest of the paper is organized as follows.

2 Background and Related Work

Recently, J. Nagi et.al. [10] studied a deep neural network approach for recognizing six different hand gestures given to a robot. Using CNNs the authors achieve a 96% accuracy rate. Then, M. Van den Bergh et.al. [3] explored the idea of using depth-sensor imagery to establish an algorithm for hand segmentation. The authors ultimately used this to recognize six different hand gestures in 3D. They achieved a 99.54% recognition rate. Some of the key components of the overall architecture were the usage of wavelets for image filtering and neural networks.

Moreover, B. Kang et.al. [5] took advantage of the recent success of CNNs for pattern recognition over images. They propose a system that makes use of depth-sensor images to study further the problem of hand gesture recognition. When recognizing signs within the same subject they averaged a 99.99% accuracy rate over five subjects. However, when recognizing signs across different subjects, their accuracy rate dropped to 83.58%.

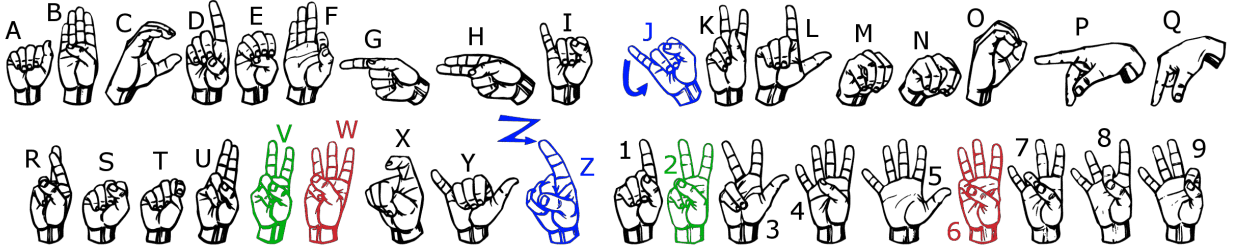


Figure 1: The American Sign Language (ASL) displaying 26 signs corresponding to the English alphabet (A to Z) and 9 signs for numbers (1 to 9).



Figure 2: Examples of ASL hand gestures corresponding to the number one and number two with variations in the horizontal axis and its inclination with respect to a depth-sensor camera.

Our research aims to further study the problem posed in [5] of increasing accuracy rates over different subjects. In the next section we discuss the dataset used and propose a deep learning approach using autoencoders and a neural network.

3 Methodology

3.1 Data

This research focuses in the ASL as a case study [2]. The ASL has 26 hand gestures corresponding to the letters in the English alphabet; it also contains 9 hand gestures for every single number. Figure 1 depicts the gestures pertaining to our study.

We use the data provided in [5] that was released in 2015. This dataset consists of images acquired with a three-dimensional depth-sensor camera. There is a total of 31,000 images available with a resolution of 256×256 . The images correspond to already segmented dept-images that contain the area of the hand. The authors use a rather simple algorithm to make the segmentation based on the fact that in all depth images the hand is the closest object with respect to the camera.

Not all the 35 signs (26 letters and 9 numbers) were considered in this study. Some signs were excluded and others considered jointly as follows.

The signs corresponding to J and Z clearly require a sequence of images rather than a single instance, as can be seen in Figure 1. This goes beyond the scope of this project; although the detection of signs from live-video sequences is part of a bigger project, we will not address it in this paper. For that reason these two signs were excluded.

The signs corresponding to V and 2, by observation, are nearly identical and their distinction requires contextual information. Similarly, the signs for letter W and number 6 require being interpreted in context. For this reason, these signs were considered as the same sign, leaving a total of 31 signs.

There is a total of five different subjects and each subject produced 200 images of each sign. This represents a total 1,000 images per sign and 31,000 images overall. The images collected capture each subject making a hand gesture moving across the horizontal axis and varying inclination of the hand gesture, as depicted in Figure 2.

3.2 Sparse Autoencoders

A sparse autoencoder is usually categorized as a neural network with unsupervised learning [6]. In a general sense an autoencoder is trained to output an approximation of the input provided a deep architecture of layered neurons that encode and decode based on the input stimuli. In our research we use a sparse autoencoder that specifically minimizes a modified loss function based on the mean squared error.

Let $\mathbf{x} \in \mathbb{R}^d$ be a d -dimensional input vector. Then the loss function of the common sparse autoencoder is defined as follows:

$$L = \frac{1}{N} \|\mathbf{x}_n - \hat{\mathbf{x}}_n\|_2^2 + \theta_w \frac{1}{2} \sum_{l=1}^L \|\mathbf{w}^l\|_2^2 + \theta_s \sum_{m=1}^M KL(\theta_\alpha \|\bar{\alpha}_m) \quad (1)$$

where N is the total number of training samples; $\hat{\mathbf{x}}_n$ is the learned (or encoded) approximation of the n -th input vector \mathbf{x}_n ; θ_w controls the sparseness of the weights of the network, $\mathbf{w} \in \mathbb{R}^d$; L denotes the number of layers in the deep network; θ_s regulates the sparsity of the activation functions' output, α , in every neuron in the network; M is the total number of neurons in the deep network; and $KL(\cdot)$ is the Kullback-Leibler divergence function [4] used to measure how much the observed average activation of the m -th neuron, $\bar{\alpha}_m$, actually deviates from the desired average output, θ_α .

The Kullback-Leibler divergence function can be defined as follows [11]:

$$\sum_{m=1}^M KL(\theta_\alpha \|\bar{\alpha}_m) = \sum_{m=1}^M \theta_\alpha \log\left(\frac{\theta_\alpha}{\bar{\alpha}_m}\right) + (1 - \theta_\alpha) \log\left(\frac{1 - \theta_\alpha}{1 - \bar{\alpha}_m}\right) \quad (2)$$

where the average output of the m -th neuron, $\bar{\alpha}_m$, at the l -th layer is given by

$$\bar{\alpha}_m = \frac{1}{N} \sum_{n=1}^N \psi\left(\mathbf{w}_m^{(l)T} \mathbf{x}_n + b_m^{(l)}\right) \quad (3)$$

where $\psi(\cdot)$ is the neuron's activation function, and $b_m^{(l)}$ is the bias term for the m -th neuron at the l -th layer. In this research we specifically use logistic (sigmoid) activation functions, $\psi(z) = 1/(1 - e^{-z})$, for any given value of z .

By observing the mathematical form of (1), it is feasible to apply an accelerated form of guided learning known as scaled conjugate gradient (SCG) descent [8]. SCG has proven to be a reliable and efficient form of minimizing loss functions such as the one for the sparse autoencoder, overcoming the shortcomings of a traditional conjugate gradient and a back-propagation with gradient descents [6].

3.3 Deep Learning Architecture

Two stacked autoencoders are combined with a feedforward neural network in a five-layer architecture, as shown in Figure 3. The first two layers are a set of unsupervised autoencoders that minimize the loss function in (1). The first layer, i.e., an encoding layer, receives as input N images of 256×256 as row vectors, each denoted as $\mathbf{x}_n \in \mathbb{R}^{65536}$, where $n \in \{1, 2, \dots, N\}$. The training phase encodes the attributes using 100 neural units to produce $\hat{\mathbf{x}}_n \in \mathbb{R}^{100}$, and decodes back to the feature space using, intuitively, 65536 neural units; all neural units use logistic activation functions.

Similarly, the third and fourth layers are an encoder and decoder, respectively. The encoder in the third layer receives as input an encoded version of the input coming from the first layer, denoted as $\hat{\mathbf{x}}_n$, and encodes using 50 neural units producing a modified version of the feature vector denoted as $\tilde{\mathbf{x}}_i \in \mathbb{R}^{50}$. The decoder in the fourth layer decodes using 100 neural units.

In the last layer of the model we use a network of 31 neural units with softmax activation functions. Each neuron is stimulated $\tilde{\mathbf{x}}_n$ and is trained to predict the probability of the n -th sample belonging to a specific class $C \in \{1, 2, \dots, 31\}$. The output of this layer for the n -th sample is the estimated probability of that sample belonging to all classes, formally denoted as $\hat{\mathbf{d}}_n \in \mathbb{R}^{31}$. The layer is trained to minimize the cross entropy function [14] given by:

$$E = \frac{1}{N} \sum_{n=1}^N \sum_{c \in C} \hat{d}_{cn} \ln d_{cn} + (1 - \hat{d}_{cn}) \ln(1 - d_{cn}) \quad (4)$$

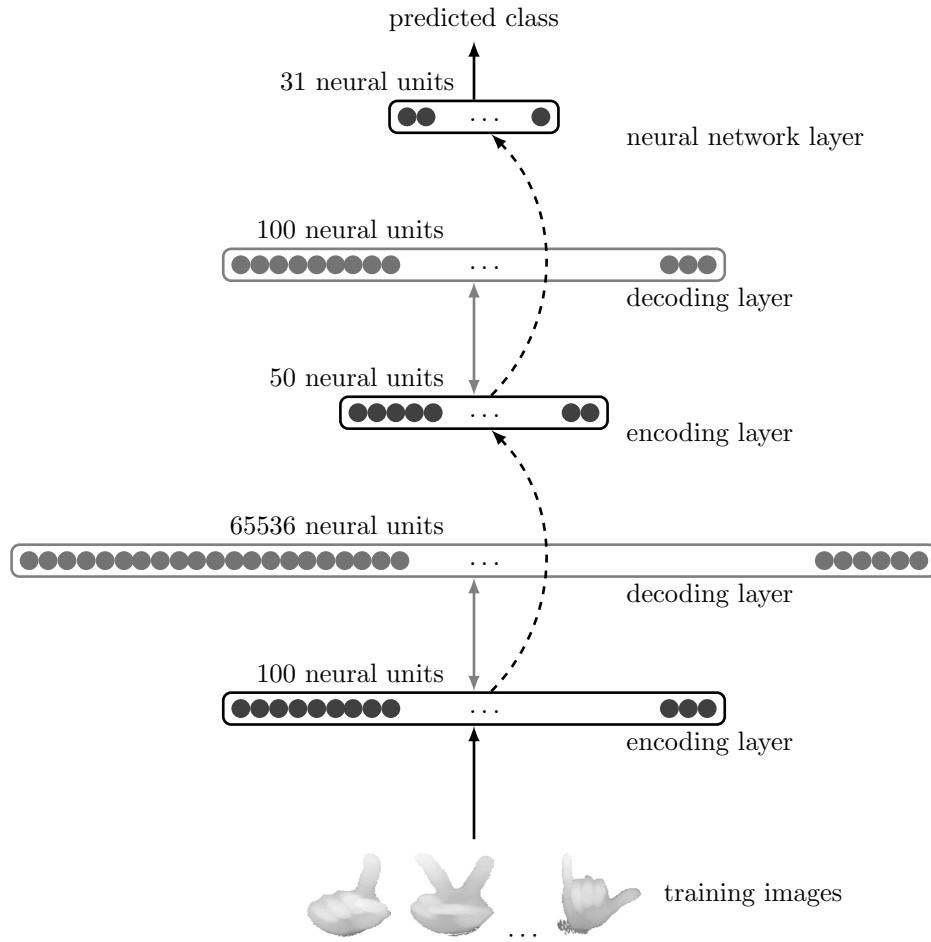


Figure 3: Deep architecture during training. The training begins with the first two layers, encoder - decoder, and once the training is complete feature are encoded and propagated to the third layer in order to further encode - decode high-level features. Finally, the last neural layer retrieves the encoded features from the third layer and learns the target class. The training is performed using SCG descent [6].

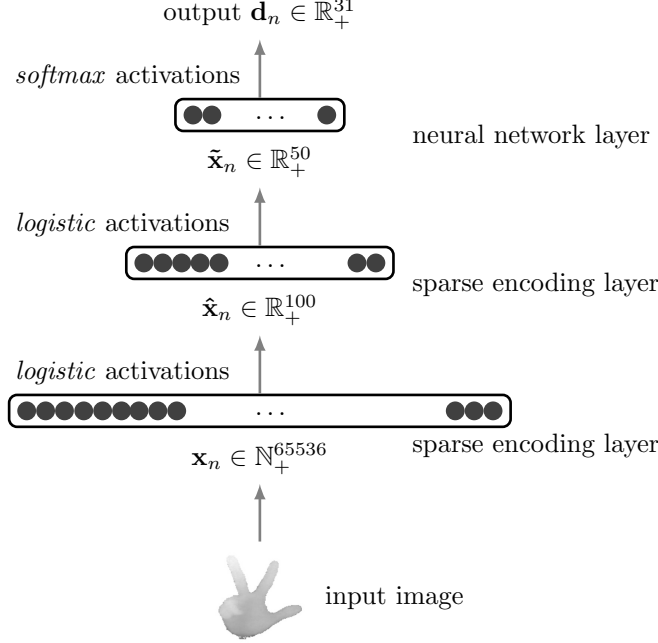


Figure 4: The working architecture when testing the system. The input is any test image which is passed through the first sparse encoder in the stack, reducing the dimensionality of the problem to 100. In the second sparse encoder the feature space is further reduced to 50. The output are probabilistic outputs corresponding to each of the 31 classes.

where $\mathbf{d}_n \in \mathbb{R}^{31}$ is the true probability of the n -th sample belonging to a specific class.

Once the process of training the autoencoders and the softmax layer, the network undergoes a last refined training phase. In this last process, only the first, third, and fifth layers are fully connected and trained simulating a feed-forward neural network, as shown in Figure 4. The initial weights are those obtained during the encoding-decoding learning phase and fine tuned using SCG descent to minimize the cross entropy in (4).

4 Experiments

4.1 Setup

The experimental setup was as follows. The dataset was divided in 50%, 25%, and 25% for training, testing, and validation respectively. Two autoencoders were trained using SCG to minimize the cross entropy previously defined. The first autoencoder has 100 neurons and the second one has 50. The second autoencoder is trained with the reduced features from the first autoencoders. A softmax neural network is then trained to minimize the mean squared error with SCG.

The process is done once per each subject to match the experiments done by Kang et. al. in [5]. The data was not processed in any other manner before being presented to the neural architecture for training nor testing. Thus, the inputs are row-vector versions of 8-bit depth images as shown in Figure 2.

4.2 Results and Discussion

Performance results on the validation sets are shown in Table 1. The table indicates that the average accuracy was of 98.9% which is similar to the results reported in [5] of 99.9%. Although the difference is 1%, it is not statistically significant. Furthermore, the deep architecture proposed in this paper is more efficient than the CNN proposed by the authors. The accuracy (ACC) is calculated as $\frac{TP+TN}{TP+FP+TN+FN}$ where TP is the count

Table 1: Performance of the deep architecture over the validation sets.

	S1	S2	S3	S4	S5	Avg.
ACC	0.9748	0.9923	0.9935	0.9929	0.9910	0.9889
SPC	0.9991	0.9997	0.9998	0.9998	0.9997	0.9996
MAE	0.1483	0.0640	0.0373	0.0347	0.0494	0.0667

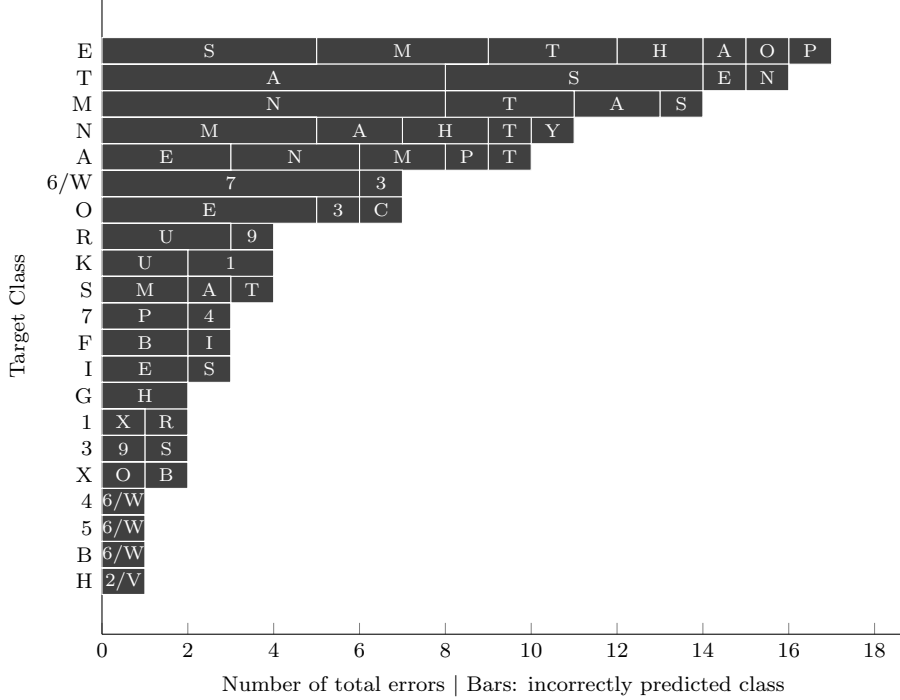


Figure 5: Stacked bar chart of classification errors. Every stacked bar indicates the predicted class and the size indicates frequency amount. Common errors are with hand signs that involve a closed hand gesture.

of true positives, TN is the count of true negatives, FP is the count of false positives, and FN is the count of false negatives. When it comes to specificity (SPC), defined as $\frac{TN}{FP+TN}$, the proposed model gives a measure of 0.99, indicating that the model is very good at predicting true negatives. This quality is desired in this type of problems to make sure the model is sure what a sign is not. This property could be attributed to the minimization of the Kullback-Leibler divergence function defined in (2) that causes the average outputs of the neural units to be low. Similarly, a low mean absolute error (MAE), defined as $\frac{1}{N} \sum_{i=1}^N |d_i - \hat{d}_i|$, is an indicator of low average error and low uncertainty in the output of the neural units. The average MAE was 0.06 and it was as low as 0.03 for some subjects.

Figure 5 shows all the errors made after training over the validation set. The figure indicates that the most common error is with the sign for the letter 'E' which is confused with the letters 'S', 'M', and 'T'. A close inspection of Figure 1 reveals that these signs are very similar and these errors are not surprising. Similarly, the sign 'M' was misclassified as 'A' and 'S'. Most misclassifications in Figure 5 are related to signs done when the hand is making a fist form and the differences in depth are low.

To illustrate this further, Figure 6 shows a variety of misclassification errors. From the figure it can be seen that hand gestures with a closed fist can be confused with other similar gestures. However, a close inspection of other gestures suggests that errors are also caused by poor segmentation of the hand area. For example, consider the signs corresponding to numbers '4' and '6', and also letters 'E', 'A', and 'M', the lower portion of the image has a section that was not segmented out of the image and it has been introduced as part of the input. It is possible that the network encoded this as a distinctive feature of the images leading

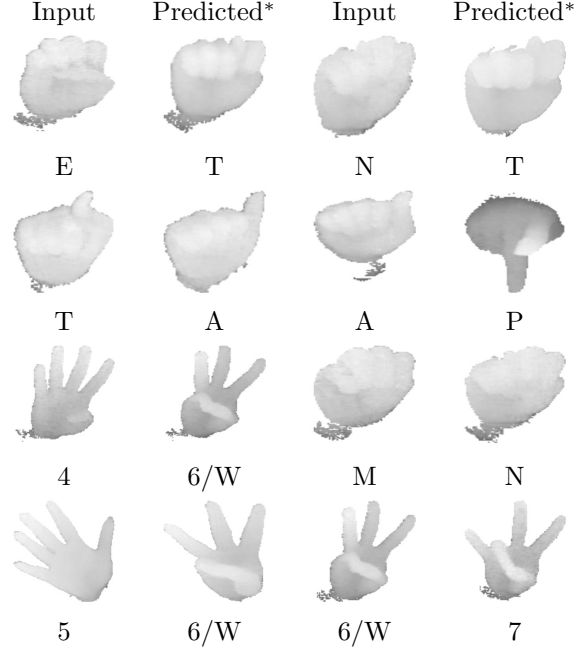


Figure 6: Examples of classification errors. *The image shown as predicted is the nearest neighbor found in the predicted class with respect to the input.

to classification errors. Figure 7 visualizes the weights associated to each neural unit in the first encoding layer for the fifth subject. The weights are capturing higher-level features and at the same time some seem to discard information around the limits of the images, but some seem to rely on regions of the image that are consistent with regions where images exhibit poor segmentation. Further studies are required to confirm this, however.

As shown in Table 1, the overall accuracy is 98.9%, and furthermore, Figure 8 shows the average accuracy for each individual sign. From the figure it can be seen that signs that involve hand gestures are likely to have lower accuracy. The figure also shows that about half of the signs achieve perfect classification over samples that were unseen by the network architecture. This indicates superior generalization abilities of the proposed deep architecture.

References

- [1] Al-Jarrah, O., Halawani, A.: Recognition of gestures in arabic sign language using neuro-fuzzy systems. *Artificial Intelligence* 133(1-2), 117–138 (2001)
- [2] Baker, C., Cokely, D.: *American sign language. A Teacher’s Resource Text on Grammar and Culture*. Silver Spring, MD: TJ Publ (1980)
- [3] Van den Bergh, M., Van Gool, L.: Combining rgb and tof cameras for real-time 3d hand gesture interaction. In: *Applications of Computer Vision (WACV)*, 2011 IEEE Workshop on. pp. 66–72. IEEE (2011)
- [4] Joyce, J.M.: Kullback-leibler divergence. In: *International Encyclopedia of Statistical Science*, pp. 720–722. Springer (2011)
- [5] Kang, B., Tripathi, S., Nguyen, T.Q.: Real-time sign language fingerspelling recognition using convolutional neural networks from depth map. In: *Pattern Recognition (ACPR)*, 2015 3rd IAPR Asian Conference on. pp. 136–140. IEEE (2015)

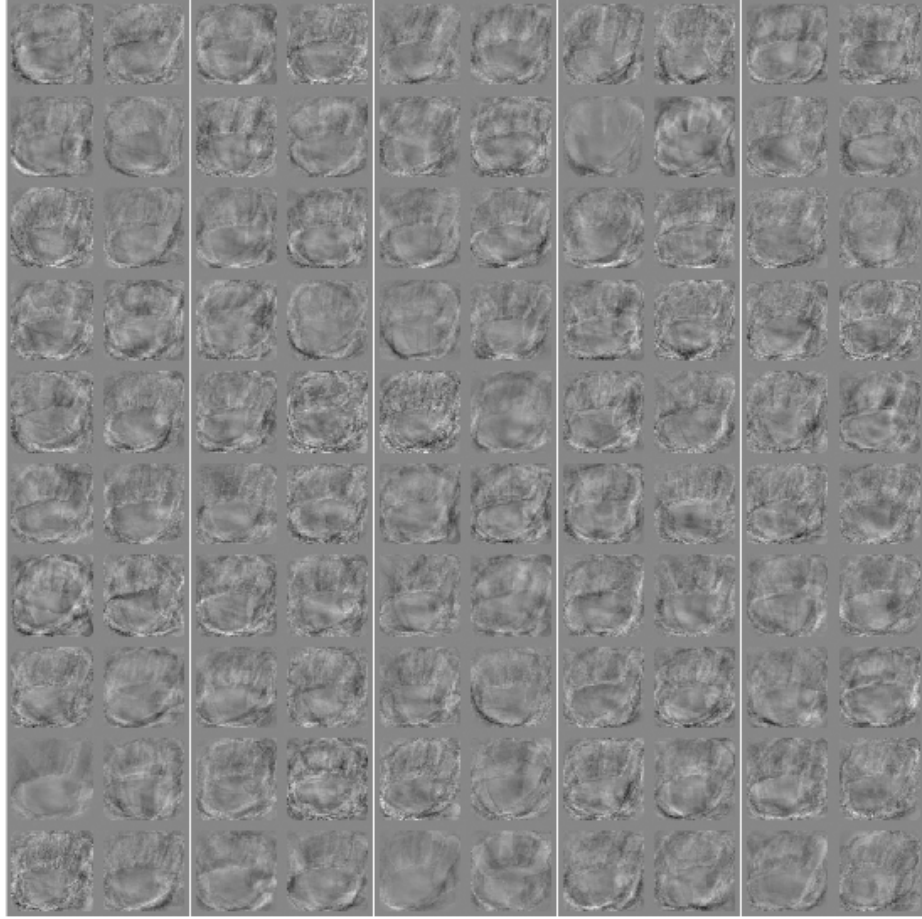


Figure 7: Weights associated with 100 trained neurons in the first layer for the fifth subject.

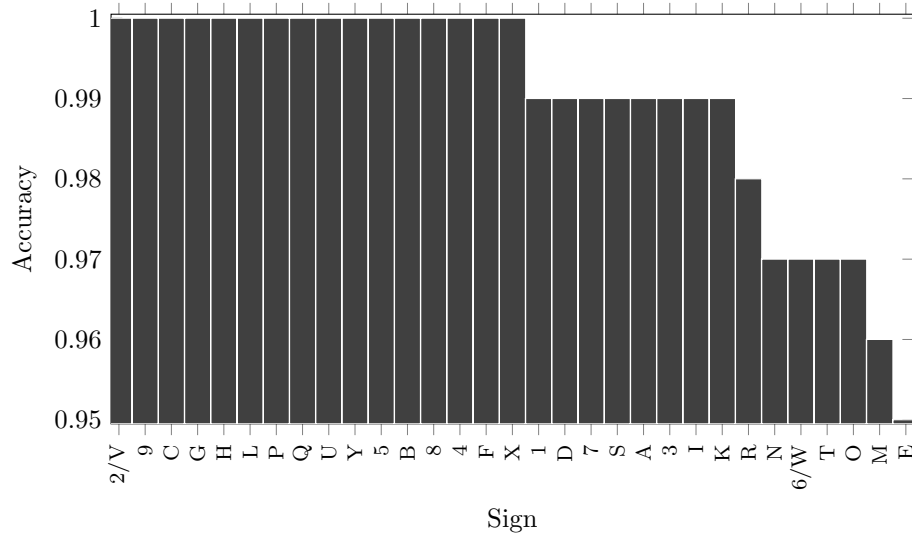


Figure 8: Average accuracy for each different sign on validation set. Most signs with lower accuracy are ones whose sign involves a closed hand gesture.

- [6] Le, Q.V.: Building high-level features using large scale unsupervised learning. In: Acoustics, Speech and Signal Processing (ICASSP), 2013 IEEE International Conference on. pp. 8595–8598. IEEE (2013)
- [7] Lichtenauer, J.F., Hendriks, E.A., Reinders, M.J.: Sign language recognition by combining statistical dtw and independent classification. *IEEE Transactions on Pattern Analysis and Machine Intelligence* 30(11), 2040–2046 (2008)
- [8] Møller, M.F.: A scaled conjugate gradient algorithm for fast supervised learning. *Neural networks* 6(4), 525–533 (1993)
- [9] Murthy, G., Jadon, R.: A review of vision based hand gestures recognition. *International Journal of Information Technology and Knowledge Management* 2(2), 405–410 (2009)
- [10] Nagi, J., Ducatelle, F., Di Caro, G.A., Cireşan, D., Meier, U., Giusti, A., Nagi, F., Schmidhuber, J., Gambardella, L.M.: Max-pooling convolutional neural networks for vision-based hand gesture recognition. In: Signal and Image Processing Applications (ICSIPA), 2011 IEEE International Conference on. pp. 342–347. IEEE (2011)
- [11] Olshausen, B.A., Field, D.J.: Sparse coding with an overcomplete basis set: A strategy employed by v1? *Vision research* 37(23), 3311–3325 (1997)
- [12] Starner, T., Pentland, A.: Real-time american sign language recognition from video using hidden markov models. In: Motion-Based Recognition, pp. 227–243. Springer (1997)
- [13] Starner, T., Weaver, J., Pentland, A.: Real-time american sign language recognition using desk and wearable computer based video. *IEEE Transactions on Pattern Analysis and Machine Intelligence* 20(12), 1371–1375 (1998)
- [14] Szegedy, C., Vanhoucke, V., Ioffe, S., Shlens, J., Wojna, Z.: Rethinking the inception architecture for computer vision. In: Proceedings of the IEEE Conference on Computer Vision and Pattern Recognition. pp. 2818–2826 (2016)